LCC – 0048 11//00
CBP Tech Note-216

Linear Collider Collaboration Tech Notes

Damping Ring Design for NLC at 180 Hz Repetition Rate

November 2000

Andrzej Wolski

Lawrence Berkeley National Laboratory
Berkeley, CA

Abstract: An increase of the NLC repetition rate from 120 Hz to 180 Hz while keeping other interaction point parameters unchanged will require changes in the design of the damping rings to provide an increased damping rate. In this note, we describe an initial lattice design for a ring that provides the required damping at 90 Hz. Two such rings, operated in series or in parallel, would provide the required damping for a 180 Hz repetition rate.

CBP Tech Note-216
LCC-0048

Damping Ring Design for NLC at 180 Hz Repetition Rate

Andrzej Wolski
Lawrence Berkeley National Laboratory

October 20th, 2000

Abstract

An increase of the NLC repetition rate from 120 Hz to 180 Hz while keeping other interaction point parameters unchanged will require changes in the design of the damping rings to provide an increased damping rate. In this note, we describe an initial lattice design for a ring that provides the required damping at 90 Hz. Two such rings, operated in series or in parallel, would provide the required damping for a 180 Hz rep rate.

1 Introduction

The increase of the NLC rep rate from 120 Hz to 180 Hz requires a redesign of the damping rings to achieve a shorter damping time. There are several approaches to this work; in this note, we describe a lattice that may be considered an initial design for a damping ring operating at 90 Hz. Two such rings, operated in series or in parallel, would achieve the required damping for a 180 Hz rep rate. We do not attempt a rigorous analysis of the parameter space leading to an optimized choice of lattice parameters, as has been presented elsewhere[1], but rather present a lattice design resulting from a partially systematic approach to damping ring design. Our intention has been to produce a lattice that meets most of the major requirements for a damping ring, and that can act as a baseline for further work to improve and refine the design.

Recent work has shown the benefits of including a gradient in the main dipoles, particularly in respect of the dynamic aperture[2]. However, for the present work we use dipoles with no field gradient. Gradient bends are undesirable from a practical point of view, since they give tighter tolerances on magnet alignment, and the aim here has been to see what may be achieved without gradients in the dipoles. Also, it is known that the damping wiggler is likely to have significant impact on the nonlinear dynamics of the lattice. For the present, though, we model the dipole as a sequence of drifts and dipoles, i.e. as a linear element.

2 Design Process

A systematic approach to the design of damping rings, with particular reference to the NLC, has been described by Emma and Raubenheimer[1]. In the design of the present lattice, we adopted their general approach, which is to fix the principal parameters successively, based on the input and required output beam properties and general relationships derived between the various parameters.

2.1 Energy and Lattice Structure

We have not re-examined the choice of machine energy, which is decided by consideration of circumference, magnet design, collective effects, spin polarization and operating costs. The energy used for this and recent studies is 1.98 GeV. Also, the arguments in favor of a TME structure in the arcs are compelling, and we see no way to achieve the required emittance by opting, say, for a TBA structure, without significantly increasing the circumference.

2.2 Emittance

The natural emittance of a lattice constructed entirely from TME cells is given by the standard formula:

$$ge_0 = \frac{C_q g^3 q^3}{12\sqrt{15} J_x}$$

The properties of the extracted beam fix the required natural emittance to be below 3.0 mm mrad, and assuming the cells to be perfectly tuned, the above formula gives the bending angle per dipole as 0.1842, or a minimum of 35 dipoles. Some detuning, required to improve the dynamics of the lattice, will give an emittance increase, and we expect the wiggler to give a reduction. Our design uses 34 complete TME cells in the arcs, and four half dipoles in the matching cells to the straights.

2.3 Store Time, Damping Time and Number of Trains Stored

The store time, N_t, is the length of time each bunch train remains in the damping ring, in units of the damping time. The extracted vertical emittance is given by:

$$ge_{y,ext} = ge_{y,inj} \mathrm{e}^{-2N_t} + \frac{k}{1+k} ge_0 \left(1 - \mathrm{e}^{-2N_t}\right)$$

where k is the coupling. Emma and Raubenheimer[1] discuss considerations leading to a choice for N_t. The considerations include the alignment tolerances on the lattice. A value of approximately 4.8 is appropriate. For a given store time and machine rep rate, the damping time is proportional to the number of bunch trains stored:

$$t_y = \frac{N_{trains}}{f_{rep} N_t}$$

Previous studies have focused on three stored trains at a rep rate of 120 Hz. If the rep rate is effectively reduced to 90 Hz (by having two rings operating at 180 Hz), then the number of trains can be reduced to two, with only an approximate 10% drop in the required damping time. However, the reduction in circumference accompanying the cut in the number of stored trains, has a significant impact on the damping time, and allows a corresponding reduction in wiggler length. For a rep rate of 180 Hz, assuming two bunch trains stored in each of two damping rings for 4.8 damping times, the required damping time is 4.6 ms.

2.4 Circumference

In the NLC, the bunch trains will be 95 bunches long, with a bunch separation of 2.8 ns. Allowing for kicker rise/fall times of 65 ns, the space required per bunch train in the damping ring is 98.39 m. For two bunch trains, therefore, we choose a circumference

close to 200 m. The required damping time as a function of the number of trains stored, and of the machine rep rate, is shown in Figure 1.

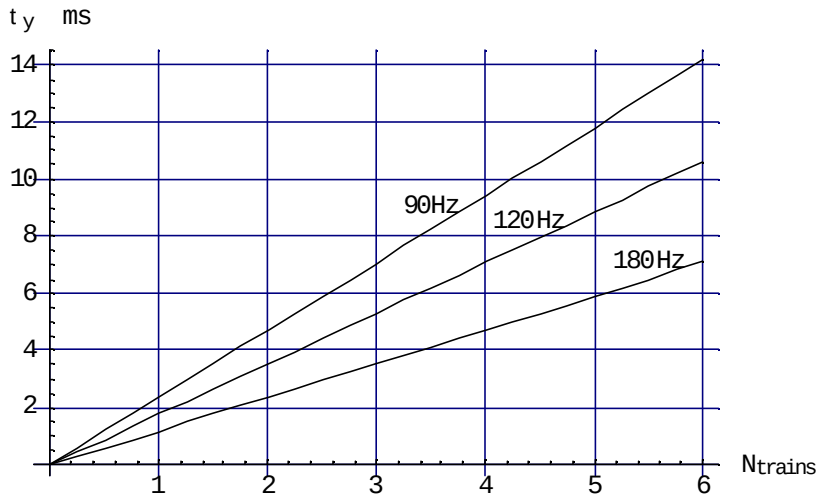

Figure 1

Required damping time as a function of number of trains stored.

2.5 Dipole Field and Wiggler Integrated Field

The (vertical) damping time of the ring is given by:

$$t_y = \frac{2E}{J_y (U_0 + U_w) f_0}$$

where U_0 is the energy loss per turn from the dipoles:

$$U_0 = C_g E^3 ecB_0$$

U_w is the energy loss per turn from the wiggler:

$$U_w = \tfrac{1}{2p} C_g E^2 e^2 c^2 \int \hat{B}_w^2 \mathrm{d}s$$

and f_0 is the revolution frequency of the particles. For a given number of stored bunch trains, the damping time is fixed by the rep rate, and the injected and extracted beam parameters. With a fixed energy and circumference, therefore, the only free parameters are the dipole field and the integrated wiggler field. Figure 2 shows how these parameters are related, for any number of bunch trains (assuming minimum lattice circumference).

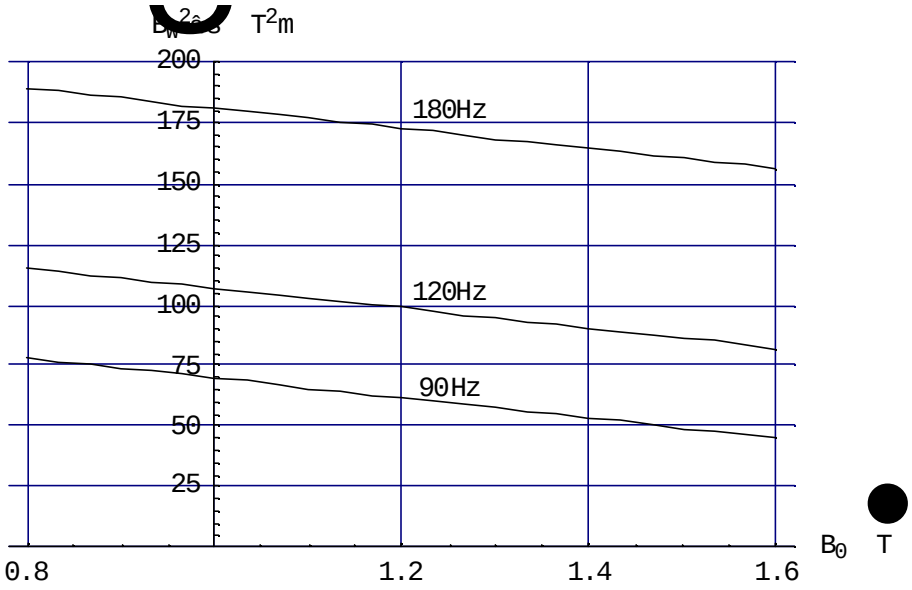

Figure 2

Relationship between integrated wiggler field and dipole field strength, assuming minimum lattice circumference for storing a given number of bunch trains.

The benefits of operating two damping rings at 90 Hz as opposed to a single ring at 180 Hz are clearly evident. There is a weaker dependence on the dipole field, with stronger fields being preferred to reduce the required strength of the wiggler. However, the dipole field also has an effect on the momentum compaction, and hence on the bunch length. In general, the momentum compaction is given by:

$$a = \oint \frac{h}{r} \mathrm{d}s$$

where the integral is taken over the whole lattice, and ρ is the local radius of curvature of the closed orbit. For the case of a TME lattice, which is tuned with

$$h = \frac{rq^2}{24}$$

in the center of the dipole, we find that

$$a = (B_0 r)\frac{q^3}{12B_0}$$

(Here we neglect the effects of the wiggler, and of detuning the cell). Hence, for a given energy and number of cells, the momentum compaction varies in inverse proportion to the dipole field. A large momentum compaction reduces sensitivity to energy errors through changes in closed orbit circumference, and reduces sensitivity to collective effects by giving a large bunch length. Emma and Raubenheimer[1] set a goal of $a \geq 5\times10^{-4}$. We select, somewhat arbitrarily, a dipole field of 1.2 T as giving a low requirement for the wiggler strength, while not pushing the momentum compaction too far below 5×10^{-4} (the final value for the momentum compaction in our lattice design is

4.35×10^{-4}. There is a dependence of the momentum compaction on the detuning factor of the cell, but this is comparatively weak.

2.6 Lattice Construction

Having selected the major parameters, we are in a position to construct the TME cell that will form the basic unit for the damping ring arcs. The additional constraints we imposed for ourselves were:

- no magnetic field gradient in the dipole;
- minimum space of 0.35 m on either side of the dipole, to allow for engineering components, radiation extraction etc.;
- minimum space of 0.40 m between adjacent quadrupoles;
- cell tuned as close as possible to the conditions for minimum emittance;
- overall length of cell as short as possible;
- phase advances horizontally and vertically controlled to give good dynamic aperture for a conceptual lattice constructed entirely from TME cells;
- beta functions and dispersion controlled to allow satisfactory correction of chromaticity, with minimum sextupole strengths.

The quadrupole component was omitted from the dipole to see what could be achieved in terms of dynamic aperture under these conditions. Note that recent work[2] has found a significant benefit of allowing some gradient in the bending magnet. Control of the phase advance in particular was problematic; for a TME cell with maximized dispersion, there is a unique relationship between the horizontal phase advance and the detuning factor. We allowed some extra flexibility by not restricting ourselves to the condition for maximum dispersion. Although this leads to stronger sextupoles for correcting chromaticity, we find in practice that the phase advance is a more significant quantity for the dynamic aperture than the strengths of the sextupoles. We discuss the issues in more detail in section 5 below. Cell structures with three quadrupoles and four quadrupoles were investigated. In practice, we found that the four-quadrupole structure gave a phase advance closer to the required value, while still allowing a compact lattice.

Having constructed the basic TME cell, we construct matching sections into the straights. The matching sections use half dipoles, as this facilitates fitting the dispersion and its gradient to zero at the end of the bending magnet.

The lengths of the straight sections are determined by the required length of the wiggler. With the parameter choices indicated above, an integrated wiggler field of a little over 60 T^2m is needed to give the required damping; assuming a peak wiggler field of 2.15 T, this gives a total wiggler length of around 26 m. The precise length of the wiggler will depend on the exact circumference and TME cell detuning. The wiggler is split into sections of 4.624 m. The quadrupoles between the wiggler sections are tuned to keep the mean value of b_x low, as this reduces the contribution of the wiggler to the natural emittance. Attempts were made to fix the phase advances over the straight sections to integer values. If achieved, this would (in the linear approximation) make the straights invisible to the particle dynamics, and the dynamic aperture of a TME cell would then effectively determine the dynamic aperture of the lattice. In practice, we achieved the control of the phase advance in the horizontal, but not in the vertical plane.

Consequently, the horizontal dynamics are little affected by the straight sections, but the vertical dynamic aperture is reduced (see the discussion below).

Lattice functions for different sections of the lattice are shown in Figure 3 through Figure 6.

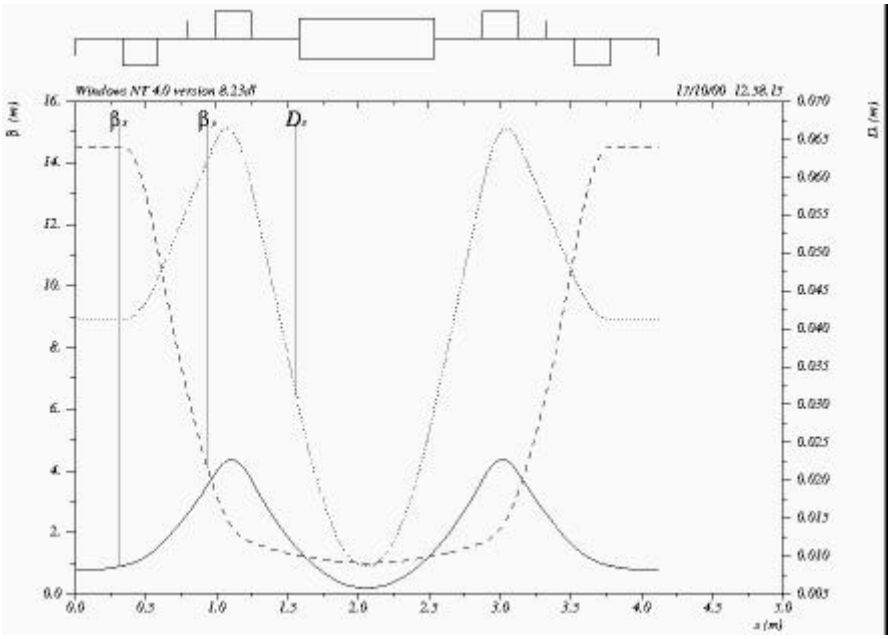

Figure 3

Lattice functions in an arc (TME) cell.

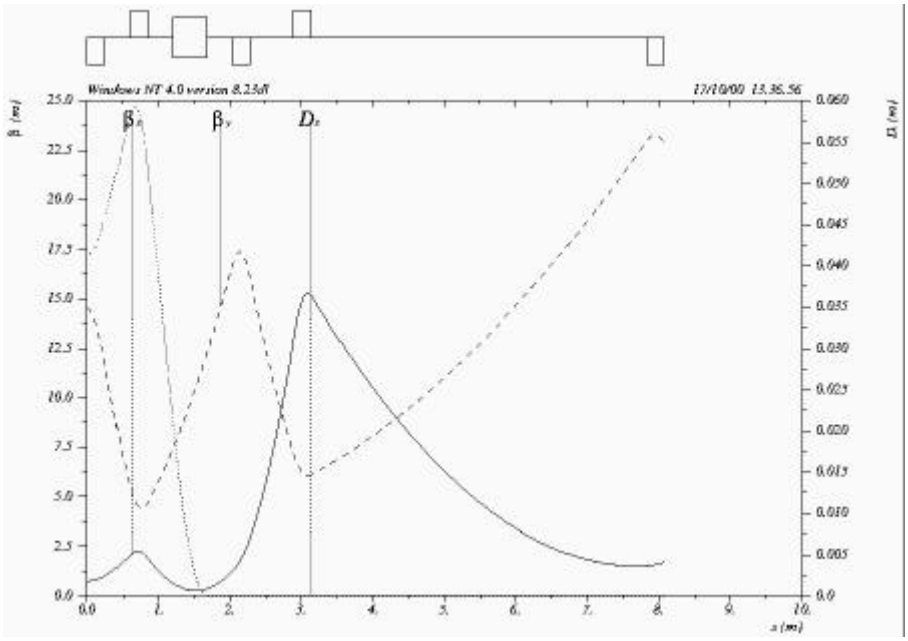

Figure 4

Lattice functions in matching cell between arc and straight section.

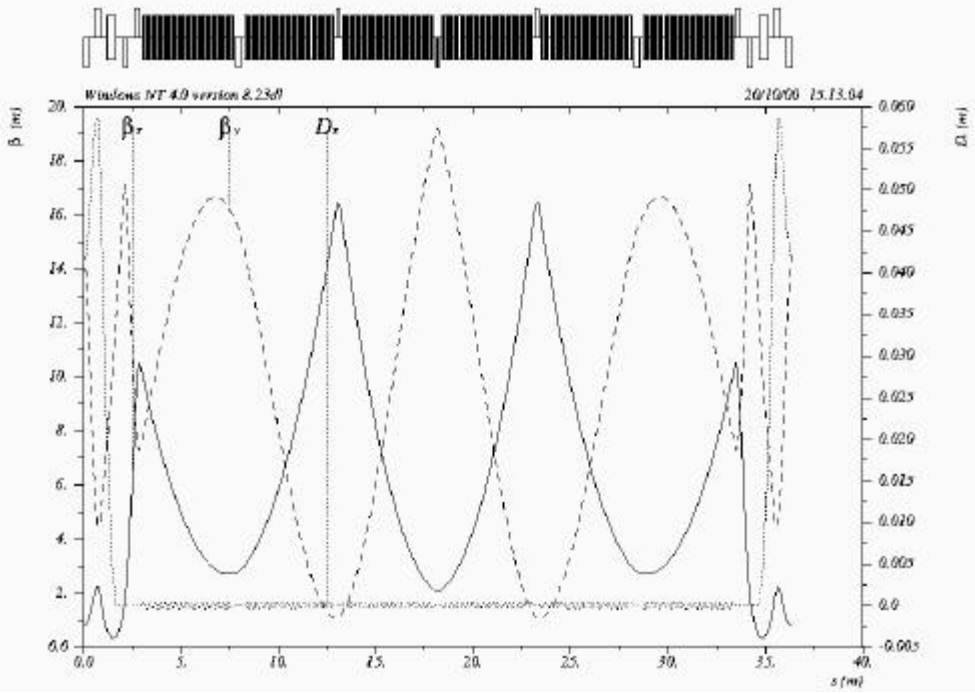

Figure 5

Lattice functions through the wiggler straight.

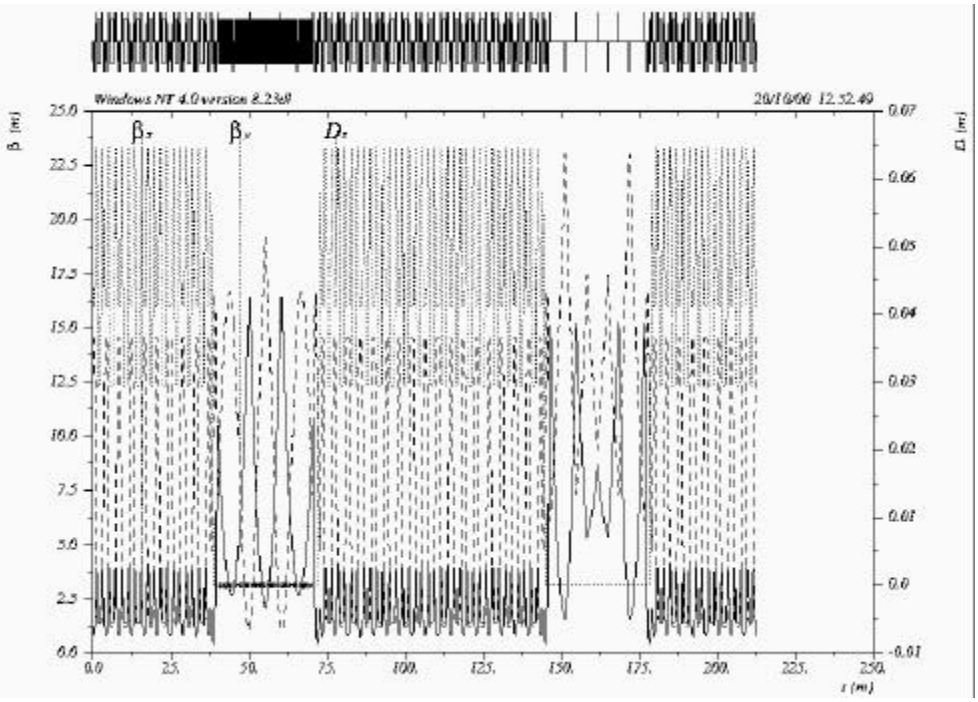

Figure 6

Lattice functions for the complete lattice.

3 Chromatic Properties

Although the sextupoles are adjusted to give zero first-order chromaticity, the tune shift with momentum can still be significant, as a result of large higher order chromaticity. The variation of horizontal and vertical tune with momentum deviations up to ±0.6% are shown in Figure 7, and the working point in tune space is shown in Figure 8. As no effort has been made so far to reduce the higher order chromaticities, the tune shifts with momentum are large, leading to a small momentum aperture.

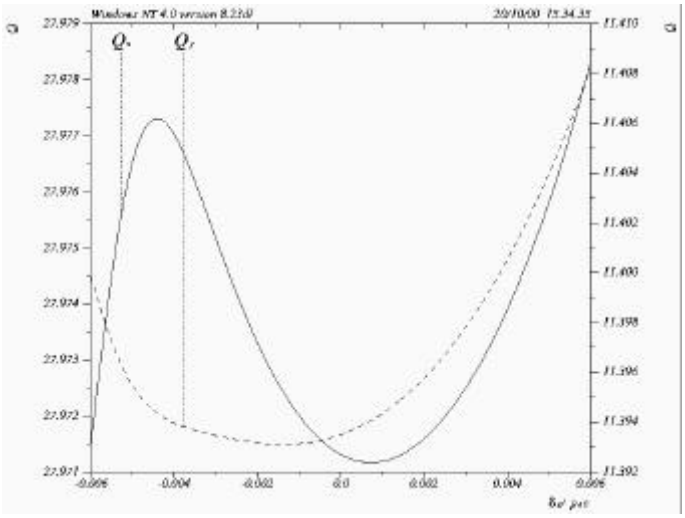

Figure 7

Variation of tunes with momentum, up to ±0.6% momentum deviation.

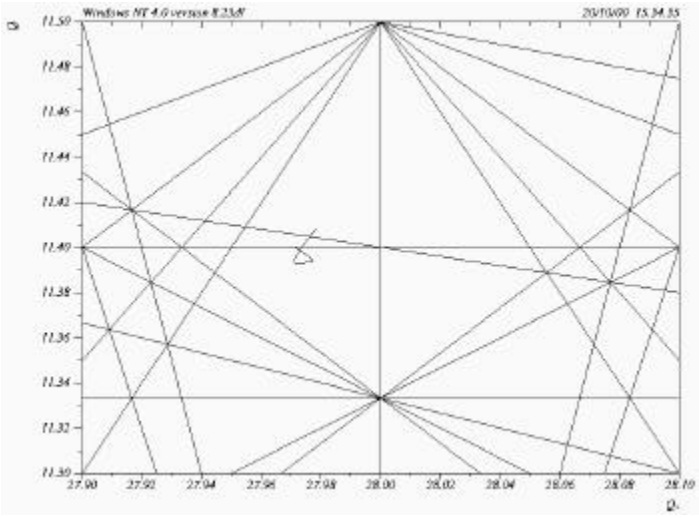

Figure 8

Working point of the lattice in tune space. The curved line near the center of the plot shows variation of the tune with momentum deviations up to ±0.6%. Resonance lines up to sixth order are shown.

We note that the lattice tunes have a strong effect on the magnet alignment tolerances, and integer and half-integer values in particular are to be avoided. In this respect, the present working point is unsuitable, since it lies close to an integer resonance.

4 Lattice and Wiggler Emittance

The minimum emittance for the lattice is achieved when the horizontal beta and dispersion functions are minimized at the centers of the dipoles, with values

$$\breve{b}_0 = \frac{L}{2\sqrt{15}} \qquad \breve{h}_0 = \frac{Lq}{24}$$

and the emittance is then

$$g\breve{e} \approx \frac{C_q g^3}{J_x} \frac{q^3}{12\sqrt{15}}$$

With a field of 1.2 T, the main dipoles in the lattice have a length of 0.96 m. The optimum lattice function values are then $\breve{b}_0$=0.124 m and $\breve{h}_0$=6.98×10^{-3} m. If the cell is detuned such that $b_0 = b_r \breve{b}_0$ and $h_0 = h_r \breve{h}_0$, then the emittance is increased by a factor[3]:

$$e_r = \frac{5h_r}{8b_r}(h_r - 2) + \frac{9}{8b_r} + \frac{b_r}{2}$$

It is straightforward to show that, for a given e_r, the maximum dispersion (and hence lowest chromatic sextupole strengths) is given by the conditions:

$$b_r = e_r \qquad h_r = 1 + 2\sqrt{\frac{e_r^2 - 1}{5}}$$

For our present lattice, in the center of the arc cell dipoles, the lattice functions take values of 0.1884 m for b_x and 0.00860 m for h_x; this results in a detuning factor $e_r = 1.11$, with b_r = 1.52 and $h_r = 1.23$. Thus, we do not satisfy the condition $b_r = e_r$ for maximum dispersion for a given detuning, and we expect the sextupoles to be rather stronger than strictly necessary. However, the values we obtain correspond to reasonable cancellation between adjacent sextupoles resulting from the phase advance. In practice, we find this a more effective way to achieve a good dynamic aperture than minimizing the sextupole strengths (see Section 5).

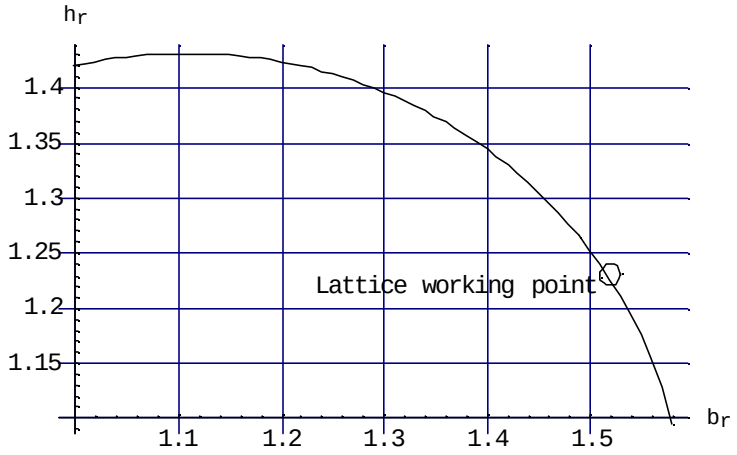

Figure 9

Lattice function relationship for a fixed detuning factor e_r =1.11. The current working point gives much lower dispersion than potentially possible for the emittance, leading to greater than necessary sextupole strengths.

The theoretical minimum normalized emittance of a 1.98 GeV lattice constructed with 36 dipoles is 2.55 mm mrad. With the detuning factor of 1.11, the natural emittance is 2.83 mm mrad (this does not include the small additional increase from the dipoles in the matching cells adjacent to the straight sections). However, with the wiggler inserted in the lattice, we find that the emittance drops to 2.35 mm mrad. The reason for this is that the emittance reduction from the wiggler's additional damping is not fully compensated by the emittance of the wiggler itself. This is readily understood if we consider the expression for the emittance of the lattice in the presence of the wiggler[1,4]:

$$ge_0 \approx \frac{C_q g^3}{12(J_x + F_w)}\left(e_r \frac{q^3}{\sqrt{15}} + \frac{\langle b_x \rangle \hat{B}_w^3 l_w^2 F_w}{16(B_0 r)^3}\right)$$

The wiggler contribution to the emittance is determined by the mean horizontal beta function, $\langle b_x \rangle$ in the wiggler, and by the ratio of energy loss in the wiggler to the energy loss in the dipoles, F_w. For a "critical" value of the mean beta function, given by:

$$\langle b_x \rangle_c = \frac{16(B_0 r)^3 e_r q^3}{\sqrt{15} J_x \hat{B}_w^3 l_w^2}$$

the emittance becomes independent of F_w. For a mean beta function below $\langle b_x \rangle_c$, increasing the length of the wiggler reduces the emittance. For the current lattice, with a peak wiggler field of 2.15 T and a period of 0.27 m, we find the critical value of the mean beta function to be 9.7 m. The actual value of the mean beta function is 6.66 m, so we are within the regime where increasing the wiggler length reduces the emittance. With an energy loss ratio F_w of 1.39, there is an emittance reduction of nearly 20%, to 2.35 mm mrad.

5 Particle Dynamics

The damping ring must have a good dynamic aperture to minimize particle loss, particularly during injection. The aperture is limited by the sextupoles, which are used in the dispersive regions (the arcs) to correct chromaticity, and tuned to give the lattice overall chromaticity of zero both vertically and horizontally. If the straight sections are assumed to contain only linear elements, and are tuned to give exact integer phase advances horizontally and vertically, then the dynamics of the lattice reduces to the dynamics of the TME cell. In the current lattice design, the fractional parts of the horizontal phase advance over both straight sections are very close to zero, while the vertically, the fractional parts are 0.0478 across the wiggler section, and 0.514 across the FODO section. The half-integer across the injection/extraction straight is a compromise, as the tune is to far from the integer to be comfortably fitted to it. As a result, we expect the dynamics of the full lattice to match closely those of the TME cell in the horizontal plane, but not necessarily in the vertical plane.

Horizontal phase space portraits are shown in Figure 10 for a single arc cell and for the full lattice. They are remarkably similar, indicating the success of the tuning of the straight sections to integer values, in the approximation where all elements in the straights are linear. The limit of stability is approximately 2.7 mm in the negative x direction, suggesting a horizontal dynamic aperture of 15 times the incoming beam size. We expect this to be adversely affected by the vertical dynamics, however.

Vertical phase space portraits are shown in Figure 11, again for a single arc cell and for the full lattice, and with the observation point at the end of an arc cell. This time we see a considerable reduction in the region of stability, with the dynamic aperture reduced from nearly 5mm (6.7 times the incoming beam size) to about 3mm (4 times the incoming beam size). This is as expected, since the vertical tunings of the arc cell and the straight sections are less likely to give stable dynamics than the horizontal tunings.

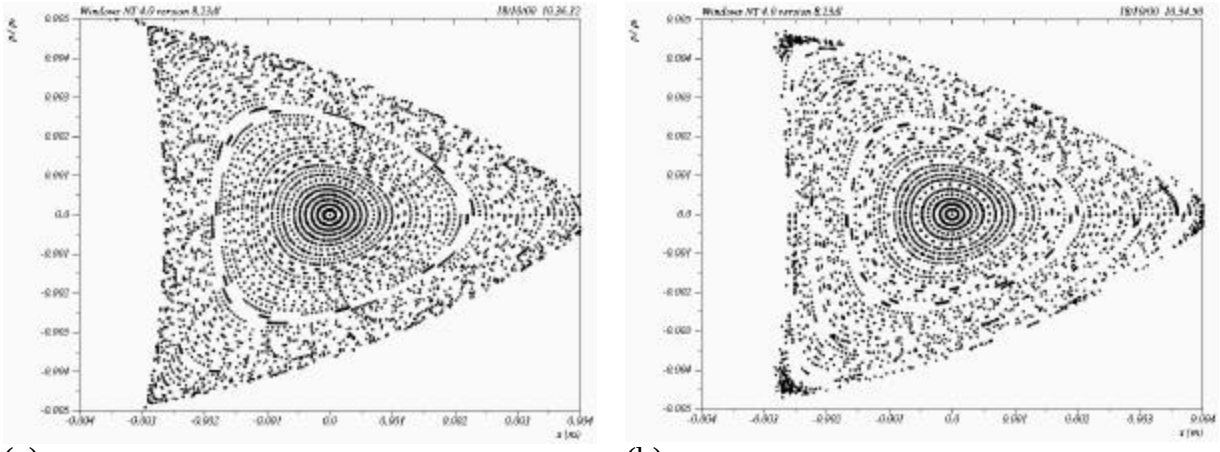

(a) (b)

Figure 10

Horizontal phase space portraits for (a) a single arc cell and (b) the full lattice. The observation point is the end of an arc cell (as shown in Figure 3) in each case, where b_x = 0.760 m.

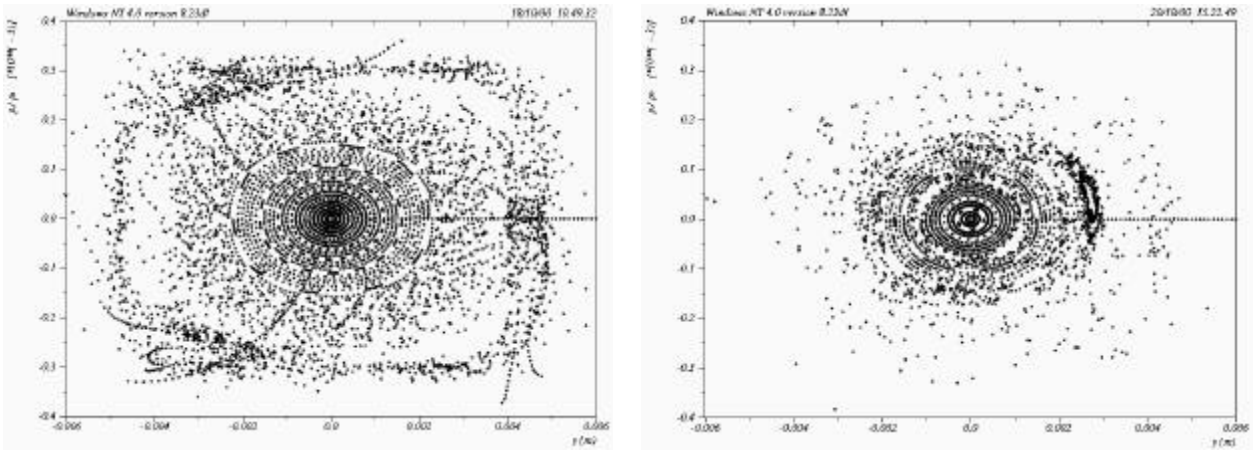

(a) (b)

Figure 11

Vertical phase space portraits for (a) a single arc cell and (b) the full lattice. The observation point is the end of an arc cell (as shown in Figure 3) in each case, where b_y = 14.53 m.

One approach to the optimization of the dynamic aperture of the TME cell is to minimize the geometric aberrations contributed by the sextupoles over each arc. This corresponds to setting the phasor sum of the sextupole kicks equal to zero, and in practice means tuning the arcs close to integer values. This kind of global correction scheme works well when one family of sextupoles is present, and less well when different families are interleaved. Also, it is generally possible only to minimize the lowest order geometric aberrations, and higher order effects may still limit the dynamic aperture to very small values. Our approach in the current lattice has been to try to arrange for exact cancellation of the geometric aberrations of the horizontally correcting chromatic sextupoles within each cell, by arranging for half-integer phase advances horizontally and vertically between these sextupoles. This leads to some compromises in the tuning of the cell, and we have in particular not adopted the conditions for maximizing the dispersion for a given detuning factor. Also, it is difficult then to arrange for cancellation of the geometric aberrations introduced by the vertically correcting chromatic sextupoles. In practice, we have been able to go some way towards what we feel are conditions for good dynamic aperture, but have not carried out a rigorous investigation of all the effects and design options. We present here some of the principal parameters and results describing the dynamic behavior of the lattice, for comparison with future studies.

The dynamic aperture for a single arc cell is shown in Figure 12, and for the full lattice in Figure 13. The observation point is the end of the TME cell as shown in Figure 3, where the values of the beta functions are 0.760 m horizontally, and 14.53 m vertically. Assuming a normalized emittance for the injected beam of 150 mm mrad horizontally and vertically, the dynamic aperture for the full lattice is 11.6 times the horizontal injected beam size, and 4 times the vertical injected beam size. This is comparable to the dynamic aperture achieved for the 120 Hz damping ring, before the gradient was introduced into the dipole[2]. We note that all tracking has been performed with "thin"

sextupoles; it is likely that tracking with elements of more realistic lengths will affect the dynamic aperture, but the effect is generally small.

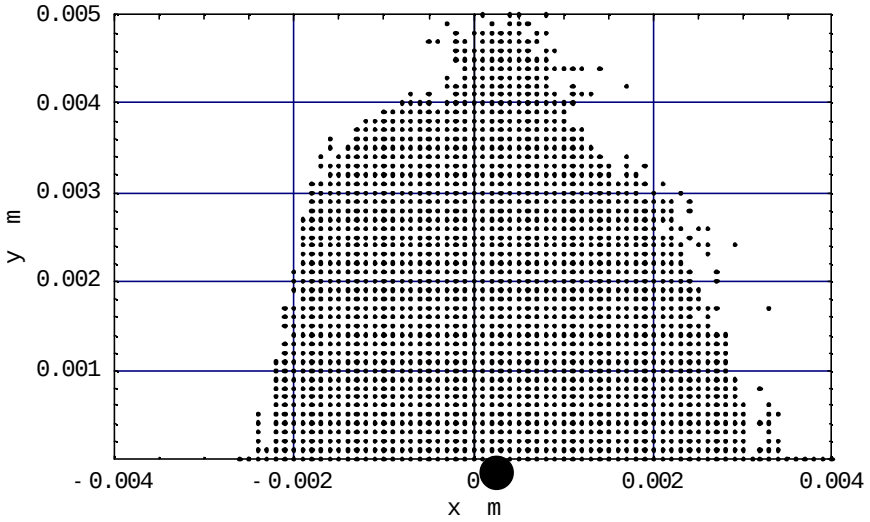

Figure 12

Dynamic aperture of a lattice constructed entirely from arc cells. The particles were tracked through 200 cells, with the observation point at the end of the arc cell, where b_x = 0.760 m and b_y = 14.53 m. The dynamic aperture is approximately $(A_x, A_y) = (14.6s_x, 6.6s_y)$.

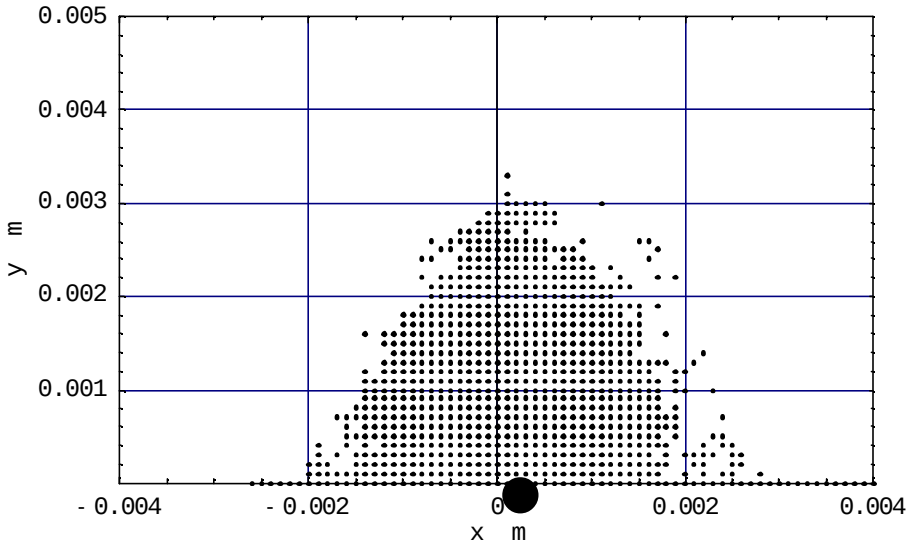

Figure 13

Dynamic aperture of the full lattice, with the wiggler modeled as a linear element. The particles were tracked through 200 turns, with the observation point at the end of the arc cell, where b_x = 0.760 m and b_y = 14.53 m. The dynamic aperture is approximately $(A_x, A_y) = (11.6s_x, 4.0s_y)$.

The dynamic aperture is limited by the nonlinearities in the arc cells, and (particularly for the vertical motion) the matching across the straight sections. Assuming that the straight sections can be modified to give more favorable phase advances, we must look at the arc cells if we are to improve the dynamic aperture significantly. At present, we limit ourselves to characterizing the arc cells in terms of the tune dependence on amplitude.

The tune shifts with amplitude in the horizontal and vertical planes are shown in Figure 14 and Figure 15 respectively. Quadratic fits are made to the data points in each case. In both cases, the tune shifts with amplitude are larger than we should like. The vertical tune hits the third integer resonance at around 4 mm vertical amplitude. The resonance is strongly driven but apparently not completely destructive at zero horizontal amplitude.

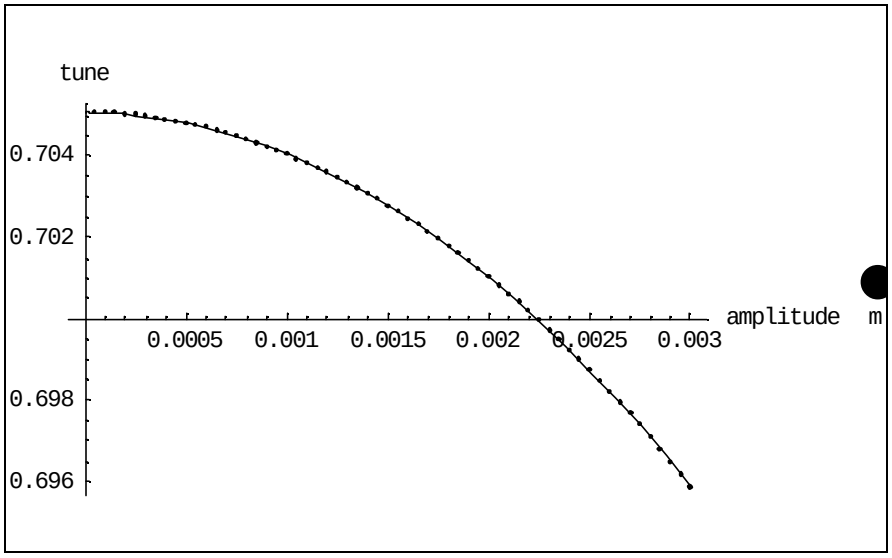

Figure 14

Horizontal tune shift with amplitude. The data points are fitted with a quadratic curve, of the form $0.7050-0.0189x-1021x^2$.

More information on the dynamics can be revealed by a frequency map analysis; this is shown in Figure 7. The plot is produced by setting up a regular grid of 4000 particles in co-ordinate space, from –2 mm to +2 mm horizontally, and from 0 mm to 3 mm vertically. The particles are tracked for 256 passes through an arc cell, and the tunes determined by Fourier analysis. Resonance lines up to ninth order are shown on the plot; the most dramatic effect is from the second order sum resonance crossing the middle of the diagram, but a ninth order coupling resonance, seen near the top of the diagram, is also driven.

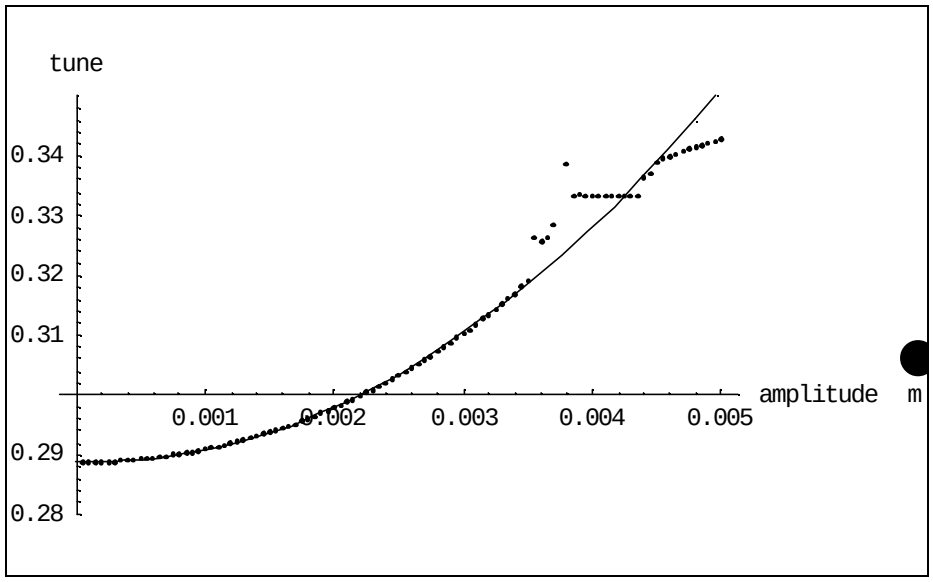

Figure 15

Vertical tune shift with amplitude. The data points are fitted with a quadratic curve, of the form $0.2889-0.869y+2656y^2$.

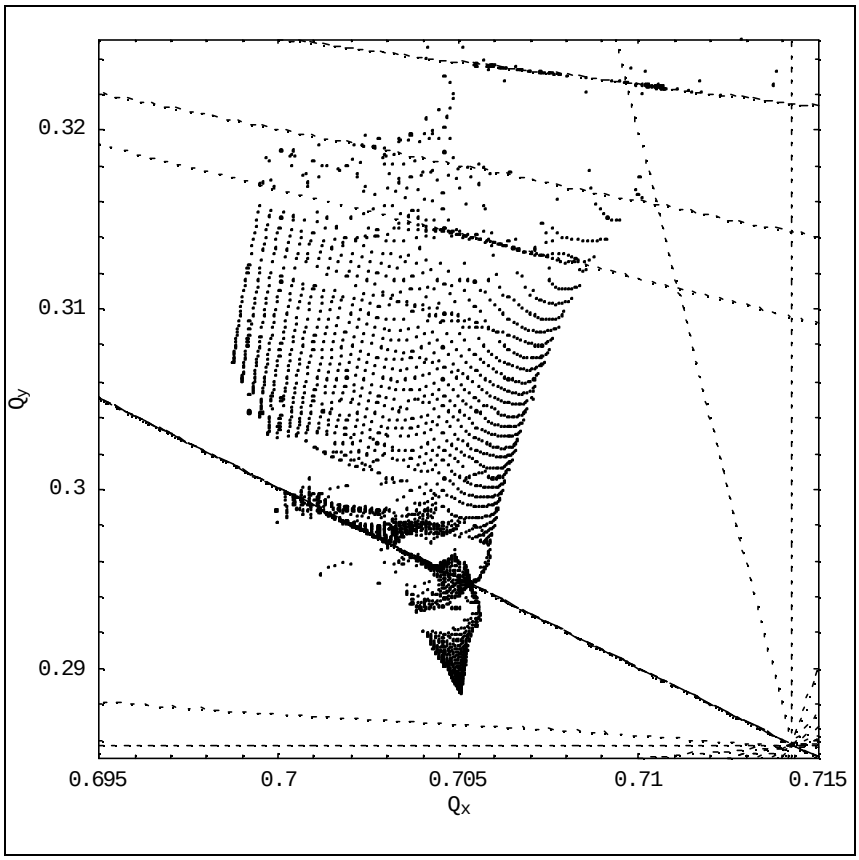

Figure 16

Frequency map analysis of an arc cell. Resonance lines up to ninth order are shown.

6 Summary of Lattice Properties

Table 1: "External" parameters.

Bunches per train	N_b	95
bunch-to-bunch spacing	t_b /ms	2.8
kicker rise/fall time	t_k /ms	65
collider repetition rate	f /Hz	180
injected horizontal/vertical emittance	ge_{inj} /mm mrad	150
extracted horizontal emittance	$ge_{x,ext}$ /mm mrad	<3
extracted vertical emittance	$ge_{y,ext}$ /mm mrad	<0.03

Table 2: Principal lattice parameters.

Energy	E /GeV	1.98
Number of bunch trains stored	N_{train}	2
Store time	N_t	4.47
Circumference	C /m	212.785
Arc cell type		TME
Arc cell length	/m	4.12
Length of each straight	/m	32.23
Number of arc cells		34 + 4×½
Normalized natural emittance	ge_0 /mm mrad	2.34
Damping times	t_x, t_y /ms	4.98, 4.97
Assumed coupling	k	0.45 %
Extracted horizontal emittance	$ge_{x,ext}$ /mm mrad	2.35
Extracted vertical emittance	$ge_{y,ext}$ /mm mrad	0.0301
Ratio of vertical equilibrium to extracted emittance	$e_{y0}/e_{y,ext}$	0.35
Momentum compaction	a	4.35×10^{-4}
RF voltage	V_{rf} /MV	1.14
RF acceptance	e_{rf}	2.4 %
Rms energy spread	s_d	0.0870 %
Bunch length	s_z /mm	3.06
Wiggler peak field	$\hat{B}_w$ /T	2.15
Wiggler period	l_w /m	0.27
Wiggler total length	L_w /m	27.744
Integrated wiggler field	$\int \hat{B}_w^2 ds$ /T^{2}m	64.12
Energy loss/turn from dipoles	U_0/keV	247

Energy loss/turn from wiggler	U_w /keV	318
Total energy loss/turn	$U_0 + U_w$ /keV	565
Energy loss ratio	F_w	1.29
Dynamic aperture	A_x, A_y	$11.6\sigma_x, 4.0\sigma_y$
Estimated momentum aperture	A_d	±0.6%

Table 3: Magnet parameters.

Main dipole length	L_0 /m	0.96
Main dipole field	B_0 /T	1.2
Main dipole bending angle	θ /deg	10
Arc quadrupole length	/m	0.25
Quadrupole pole-tip radius	/mm	0.02
Arc quadrupole pole-tip fields	/T	+1.07,-0.549

7 Future Direction

The lattice we have described above is in some respects suitable as a damping ring for the NLC operating at 180 Hz repetition rate. In particular, it meets the requirements for extracted beam emittance, and takes advantage of the fact that the damping rings will operate in pairs, to reduce the length of wiggler required in any one ring. Modifications and optimizations are needed in the following areas:

- the dynamic aperture needs to be improved, possibly by allowing a field gradient in the main dipoles, and adjusting the phase advance across the straight sections;
- the chromatic properties need to be improved, to give a larger momentum aperture;
- the lattice circumference could be reduced, by reducing the number of arc cells, to take advantage of the emittance reduction provided by the wiggler;
- the spacing between individual elements needs to be examined, to see whether the current layout is practically possible, or to see if space savings could be made;
- the effects of, and compensation schemes for, the nonlinear components of the wiggler field need to be investigated.

8 References

[1] P. Emma and T. Raubenheimer, *"A Systematic Approach to Damping Ring Design"*, September 2000.

[2] H. Nishimura, Notes on NLC Damping Ring Lattice, March – September 2000.

[3] J.P. Potier and L. Rivkin, *"A Low Emittance Lattice for the CLIC Damping Ring"*, Proceedings, PAC'97.

[4] P. Emma and T. Raubenheimer, *"Main Damping Ring Design for the NLC"*, presentation.